Improving corneal permeability of dexamethasone using penetration enhancing agents

Thareja, Abhinav; Leigh, Thomas; Hakkarainen, Jenni J.; Hughes, Helen; Alvarez-lorenzo, Carmen; Fernandez-Trillo, Francisco; Blanch, Richard; Ahmed, Zubair

DOI:
10.1016/j.ijpharm.2024.124305

International Journal of Pharmaceutics 660 (2024) 124305

Contents lists available at ScienceDirect

International Journal of Pharmaceutics

journal homepage: www.elsevier.com/locate/ijpharm

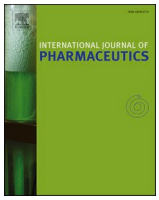

Improving corneal permeability of dexamethasone using penetration enhancing agents: First step towards achieving topical drug delivery to the retina

Abhinav Thareja [a], Thomas Leigh [b,c], Jenni J. Hakkarainen [d], Helen Hughes [e], Carmen Alvarez-Lorenzo [f], Francisco Fernandez-Trillo [b,g], Richard J. Blanch [a,h,i,j], Zubair Ahmed [a,j,*]

[a] Neuroscience and Ophthalmology Group, Institute of Inflammation and Ageing, College of Medical and Dental Sciences, University of Birmingham, Edgbaston, Birmingham B15 2TT, West Midlands, United Kingdom
[b] School of Chemistry, University of Birmingham, Edgbaston, Birmingham B15 2TT, West Midlands, United Kingdom
[c] Royal College of Surgeons in Ireland (RCSI), University of Medicine and Health Sciences, Dublin 2, Ireland
[d] Experimentica Ltd., Microkatu 1, P.O. Box 1199, 70211 Kuopio, Finland
[e] Pharmaceutical and Molecular Biotechnology Research Centre (PMBRC), School of Science & Computing, Department of Science, South East Technological University, Cork Road, Waterford City X91 K0EK, Ireland
[f] Departamento de Farmacología, Farmacia y Tecnología Farmacéutica, I+DFarma, Facultad de Farmacia, iMATUS and Health Research Institute of Santiago de Compostela (IDIS), Universidade de Santiago de Compostela, 15782 Santiago de Compostela, Spain
[g] BioMedNano Group, Centro de Investigacións Científicas Avanzadas (CICA), Facultade de Ciencias Rúa As Carballeiras, Universidade da Coruna, 15008 A Coruña, Galicia, Spain
[h] Academic Department of Military Surgery & Trauma, Royal Centre for Defence Medicine, United Kingdom
[i] Department of Ophthalmology, University Hospitals Birmingham NHS Foundation Trust, Birmingham, West Midlands, United Kingdom
[j] Centre for Trauma Sciences Research, University of Birmingham, Edgbaston, Birmingham B15 2TT, West Midlands, United Kingdom

ARTICLE INFO

Keywords:
Topical ocular drug delivery
Cornea
Penetration enhancing agents
Dexamethasone sodium-phosphate
Posterior ocular segment
Cell penetrating peptides

ABSTRACT

With an ever-increasing burden of vision loss caused by diseases of the posterior ocular segment, there is an unmet clinical need for non-invasive treatment strategies. Topical drug application using eye drops suffers from low to negligible bioavailability to the posterior segment as a result of static and dynamic defensive ocular barriers to penetration, while invasive delivery systems are expensive to administer and suffer potentially severe complications. As the cornea is the main anatomical barrier to uptake of topically applied drugs from the ocular surface, we present an approach to increase corneal permeability of a corticosteroid, dexamethasone sodium-phosphate (DSP), using a novel penetration enhancing agent (PEA). We synthesised a novel polyacetylene (pAc) polymer and compared its activity to two previously described cell penetrating peptide (CPP) based PEAs, TAT and penetratin, with respect to increasing transcorneal permeability of DSP in a rapid *ex-vivo* porcine corneal assay over 60 min. The transcorneal apparent permeability coefficients (P_{app}) for diffusion of pAc, and fluorescein isothiocyanate (FITC) conjugated TAT and penetratin were up to 5 times higher ($p < 0.001$), when compared to controls. When pAc was used in formulation with DSP, an almost 5-fold significant increase was observed in P_{app} of DSP across the cornea ($p = 0.0130$), a significant 6-fold increase with TAT ($p = 0.0377$), and almost 7-fold mean increase with penetratin ($p = 0.9540$). Furthermore, we investigated whether the PEAs caused any irreversible damage to the barrier integrity of the corneal epithelium by measuring transepithelial electrical resistance (TEER) and immunostaining of tight junction proteins using zonula occludens-1 (ZO-1) and occludin antibodies. There was no damage or structural toxicity, and the barrier integrity was preserved after PEA application. Finally, an *in-vitro* cytotoxicity assessment of all PEAs in human retinal pigment epithelium cells (ARPE-19) demonstrated that all PEAs were very well-tolerated, with IC_{50} values of 64.79 mM for pAc and 1335.45 μM and 87.26 μM for TAT and penetratin, respectively. Our results suggest that this drug delivery

* Corresponding author at: Neuroscience and Ophthalmology Group, Institute of Inflammation and Ageing, College of Medical and Dental Sciences, University of Birmingham, Edgbaston, Birmingham B15 2TT, West Midlands, United Kingdom.
E-mail addresses: a.thareja@bham.ac.uk (A. Thareja), thomasleigh@rcsi.com (T. Leigh), jenni.hakkarainen@experimentica.com (J.J. Hakkarainen), helen.hughes@setu.ie (H. Hughes), carmen.alvarez.lorenzo@usc.es (C. Alvarez-Lorenzo), f.ftrillo@udc.es (F. Fernandez-Trillo), r.j.blanch@bham.ac.uk (R.J. Blanch), z.ahmed.1@bham.ac.uk (Z. Ahmed).

https://doi.org/10.1016/j.ijpharm.2024.124305
Received 6 March 2024; Received in revised form 3 June 2024; Accepted 4 June 2024
Available online 7 June 2024

technology could potentially be used to achieve a significantly higher intraocular therapeutic bioavailability after topical eye drop administration, than currently afforded.

1. Introduction

Despite being the safest and most convenient method of ocular drug delivery, topical administration suffers from limited bioavailability of drug to internal structures beyond the ocular surface due to the presence of physiological and anatomical defensive barriers in the eye. Overall, less than 5 % of the applied amount of a drug reaches even the anterior segment tissues after eye drop administration on the ocular surface (Hughes et al., 2005; Loftsson et al., 2008; Urtti, 2006). Inflammation plays a significant role in the pathogenesis of multifactorial diseases in the posterior segment of the eye. Recent studies have demonstrated the association between inflammatory and angiogenic cascades and how either could be a cause or consequence of the other in the pathophysiology of age related macular degeneration (AMD) (Telander, 2011) and diabetic macular oedema (Romero-Aroca et al., 2016). New long term clinical management strategies include intraocular injections or implants of steroids, sometimes in combination with anti-vascular endothelial growth factor (anti-VEGF) drugs (Abadia et al., 2016).

These invasive treatments are painful to administer, cause fear and anxiety, and are financially burdensome because of the requirement for expert administration, which can lead to non-adherence and inferior visual outcomes in patients (Ehlken et al., 2020). Additionally, there is a well-documented risk of post injection complications including endophthalmitis (Sigford et al., 2015), increased intraocular pressure & glaucoma (Good et al., 2011), cataract (Thompson, 2006), and retinal tear & detachment (Karabag et al., 2015). These issues make topical drug delivery for the posterior segment a “holy-grail”. Several nanoparticulate carrier based approaches are currently being investigated extensively to achieve an effective bioavailability of drugs at the posterior segment via topical instillation (Wang et al., 2018) including lipid based solid lipid nanoparticles (SLNs) and nanostructured lipid carriers (NLCs) (Balguri et al., 2016), polymeric nanoparticles (Tahara et al., 2017), liposomes (Lai et al., 2019), etc. However, majority of them follow the scleral route instead of corneal uptake.

Penetration enhancing agents (PEAs) can facilitate increased uptake of otherwise poorly absorbed drugs into cells and across impermeable tight epithelium membranes like cornea and conjunctiva (Kaur and Smitha, 2002; Moiseev et al., 2019; Thareja et al., 2021). As opposed to nanocarrier drug delivery systems, PEAs are more versatile in their use because they do not require chemical surface processing for stability, do not need a consistent 3D shape, size or size distribution and hence are easier to scale-up, cost-effective, and do not carry the same risk of adverse health effects and hazardous environmental exposure as an obstacle in the regulatory pathway to their development (Desai, 2012). PEAs are often also used as surface coating on nanoparticles (Mahaling and Katti, 2016; Yang et al., 2019). Synthetic helical polymers are increasingly being used in drug delivery. Polyacetylene (pAc) is one such class of helical polymers that can modulate their structural conformations in response to external stimuli and their helicity can be exploited for biomembrane interactions and enhanced cargo transport across ocular barriers (Leigh and Fernandez-Trillo, 2020). We have developed a novel pAc polymer for this purpose (Fernandez Trillo and Blanch, 2023).

Cell penetrating peptides (CPPs) are short chain peptides consisting of 5–30 amino acid residues with an intrinsic ability to translocate across cell membranes through endocytic or non-endocytic mechanisms or a combination of both, which is not seen in other peptides, mainly attributable to the presence of positive charges and amphipathicity, although some anionic and hydrophobic CPPs have also been reported (Bechara and Sagan, 2013; Milletti, 2012). In a recent systematic review, we identified penetratin and TAT, as two CPPs that were the most efficient PEAs for posterior segment drug delivery (Thareja et al., 2021). TAT is a cationic CPP isolated from the Tat protein of the HIV-1 virus, whereas penetratin is a partially amphipathic CPP corresponding to the third helix of Antennapedia homeodomain protein of *Drosophila melanogaster* (Milletti, 2012; Vivès et al., 2008).

Dexamethasone sodium-phosphate (DSP) is a polar, water soluble pro-drug of dexamethasone, a corticosteroid commonly used as gold standard treatment against oedematous vascular leakage in macular oedema secondary to diabetic retinopathy (Dugel et al., 2015) or retinal vein occlusion (Haller et al., 2010), and to treat inflammation in uveitis (Saincher and Gottlieb, 2020), and sometimes as an adjunct therapy with anti-VEGF biologicals in neovascular AMD (Vakalis et al., 2015), either as intraocular injections or through sustained release intraocular implants, primarily due to its anti-inflammatory properties complemented by angiostatic and anti-permeability effects (Ciulla et al., 2004; Gaballa et al., 2021). DSP, being hydrophilic, exhibits far inferior corneal permeability compared to dexamethasone (Civiale et al., 2004).

In this study, we investigated the ability of penetratin, TAT and pAc in improving bioavailability of DSP across complex defensive ocular barriers in a medium-throughput and rapid-assay *ex-vivo* model of permeability using porcine eye tissue, developed in our group (Begum et al., 2020). pAc was synthesised using a patented protocol (Fernandez Trillo and Blanch, 2023). We first tested the permeabilities of pAc compared with that of fluorescently labelled CPPs, across porcine cornea and sclera. DSP was then formulated with pAc and non-labelled CPPs for topical application and assayed for permeability. DSP concentration in the receptor chamber was quantified using high-performance liquid chromatography (HPLC) to ascertain the enhancement in its permeability with PEAs. This was followed by safety assessment of barrier integrity of corneal epithelium using transepithelial electrical resistance (TEER) measurements and immunofluorescent staining of excised cornea with epithelial tight junction markers ZO-1 and occludin, and finally *in-vitro* cytotoxicity assessment of PEAs in human ARPE-19 cell line using the 3-[4,5-dimethylthiazol-2-yl]-2,5-diphenyltetrazolium bromide (MTT) assay. This work adds a new horizon to a safe, simple, and affordable topical ocular delivery modality of corticosteroids by modulating the transcorneal route using PEAs without causing any irreversible damage to defensive barriers of the eye, and potentially achieve therapeutic doses at the posterior segment tissues.

2. Materials and methods

2.1. PEAs

A poly(*O*-propargyl-*N*-amino carbamate) (pAc) was prepared following a proprietary, patented protocol (Fernandez Trillo and Blanch, 2023), with all the chemicals and solvents (reagent grade) purchased from Sigma-Aldrich (Poole, Dorset, UK), Fisher Scientific (Leicester, UK), VWR (Peterborough, UK), or ThermoFisher (Ashford, UK). Briefly, an acetylene monomer *O*-propargyl-*N*-(*tert*-butoxycarbonyl) amino carbamate (PBocAC) was synthesised using propargyl alcohol, carbonyldiimidazole, and *tert*-butyl carbazate in ethyl acetate. PBocAC was then polymerised upon reaction with a rhodium catalyst [Rh(NBD)B(Ph)$_4$] in tetrahydrofuran to give the protected polymer compound poly (*O*-propargyl-*N*-(*tert*-butoxycarbonyl) amino carbamate) (p(PBocAC)). p (PBocAC) was finally dissolved in trifluoroacetic acid to obtain deprotected reactive pAc polymer which was later freeze-dried to a pale-yellow powder. The protected polymer (p(PBocAC)) was characterised by gel permeation chromatography (GPC) for the following parameters: weight average molecular weight (M_w) = 41158 ± 130 g/mol, number average molecular weight (M_n) = 24615 ± 734 g/mol, and

polydispersity index (Đ) = 1.67 ± 0.04.

Freeze-dried CPPs (TAT and penetratin) used in this study were all commercially available and purchased from AnaSpec – Kaneka Eurogentec (Seraing, Belgium) and their sequences and properties are listed in Table 1.

2.2. Ex-Vivo permeability measurement of PEAs and DSP formulations in cornea and sclera

Ex-vivo Porcine Eye model: An *ex-vivo* model of permeability using porcine cornea and sclera was used to rapidly assess transcorneal and *trans*-scleral permeability, which has been established and validated by our group (Begum et al., 2020) (Fig. 1). Fresh non-scalded porcine eyes (Medical Meat Supplies, Rochdale, UK), surplus tissue from the food industry, were obtained from a local abattoir within two hours of slaughter and transported on ice in an air-tight container. The eyes were then physically examined, and those with an opaque/cloudy cornea or a visible corneal injury/scar were discarded, using only clear transparent corneas. The attached muscles and optic nerve were removed, and the globes rinsed with multiple changes of phosphate buffered saline (PBS; Cat no. BR0014G, ThermoFisher, Hampshire, UK). A small incision was made at the corneal limbus using a scalpel blade and the cornea was carefully excised with a scleral rim using curved mayo scissors. The corneal button was rinsed multiple times with PBS and placed in a petri dish containing PBS, with the corneal epithelium facing down. The remaining globe without the cornea was then cleared out of all other tissues including the lens, vitreous, retina, and choroid to obtain only the sclera, which was then rinsed thoroughly in multiple changes of PBS. 5 mm discs of cornea and sclera were excised using biopsy punches (Stiefel, GSK, Waterford, Ireland) – 3 to 4 sections from each tissue.

Corneal discs were taken from superior, inferior, nasal, and temporal cornea and each disc included both central and peripheral cornea. Each 5 mm tissue disc was then placed in a CellCrown 96 well microplate insert (Cat no. Z682004, Sigma-Aldrich, Poole, UK) with the corneal epithelium or outer sclera facing up, thus simulating eye drop instillation. The tissue disc was placed at the base of the outer insert covering the aperture and the inner insert was then placed on top of the tissue and gently pressed in to create a watertight seal without deforming the tissue. Combined inserts containing tissue discs were then placed in a black wall, clear flat-bottom 96 well microplate (Cat no. 301002, Porvair, Norfolk, UK) containing 80 µl PBS in each well. The formulation to be tested was applied into the cavity in the inner insert that acted as the donor chamber, and the concentration after diffusion through the cornea or sclera was detected in PBS in the microplate well that acted as receptor chamber.

Permeability Measurements: The PEAs were first assayed for their permeabilities at 37 °C across porcine cornea (n = 12/PEA) and sclera (n = 9/PEA). Fluorescein sodium (Cat no. 46960, Sigma-Aldrich) was used as a positive control. The 3–4 biopsy discs of cornea and sclera were randomised across all PEA groups. 20 µl each of 2.21 mg/ml (19.36 mM) polyacetylene (pAc) suspension in PBS, and 100 µM PBS solutions of N-terminal FITC labelled CPPs FITC-TAT and FITC-penetratin, and fluorescein sodium, were applied in the donor chamber and their concentrations were measured in the PBS in microplate wells after 60 min. The inserts with formulations were carefully removed from the microplates and concentration analysed in a BMG Clairostar Plus microplate reader (BMG Labtech GmbH, Ortenberg, Germany) operated using in-built Read Control acquisition software and data collected in MARS data analysis software. pAc was detected by fluorescence (λ_{ex}: 410 nm, λ_{em}: 481 nm), FITC-TAT and FITC-penetratin were detected by measuring absorbance at 496 nm and fluorescein at 488 nm. The unknown concentrations were calculated by linear regression of standard calibration curves.

Further, formulations of dexamethasone 21-phosphate disodium salt (DSP 98 %; Cat no. J64083, ThermoFisher, Oxford, UK) with PEAs were assayed for their permeability at RT across cornea (n = 12/formulation) and sclera (n = 9/formulation). The formulations were prepared in PBS as follows: 2.21 mg/ml pAc + 10 mg/ml DSP stirred overnight, 100 µM of CPPs TAT or penetratin + 10 mg/ml DSP mixed and vortexed just before use, and 10 mg/ml DSP only controls. The tissue sections were randomised as earlier and 20 µl of each formulation was applied in the donor chamber. The permeability of DSP with and without the PEAs was calculated by measuring its concentration in the receptor chamber after 60 min. The inserts were removed carefully and the solution in microplate wells was collected in micro-inserts in vials for high-performance liquid chromatography (HPLC) analysis.

HPLC for DSP Quantification: DSP transcorneal and transscleral penetration was quantified using Agilent 1260 Infinity II HPLC equipment (Agilent, Santa Clara, CA, USA) fitted with a G7129A vial autosampler, G7111B quaternary pump and G7115A diode array detector, operated and data collected by OpenLab chromatography data system (CDS) software (Agilent), using a previously published and validated method (Milojevic et al., 2002). The mobile phase consisted of a 65:35, v/v mixture of deionised water + acetonitrile (HPLC Plus, ≥ 99.9 %; Cat no. 34998, Sigma-Aldrich) adjusted to pH 2.5 with phosphoric acid (ACS reagent, ≥ 85 %; Cat no. 30417-M, Sigma-Aldrich) and degassed by vacuum filtration before running at an isocratic elution flow rate of 1 ml/min. The analytes were separated at 25 °C in an Agilent ZORBAX Eclipse Plus C18 4.6 × 250 mm reverse phase porous silica column with 5 µm particle size and 95 Å pore size (Cat no. 959990-902, USA) fitted with a 4.6 × 12.5 mm guard column (Cat no. 820950-936, Agilent). 10 µl samples were injected in each run and DSP was detected at 242 nm UV absorbance after 3.8 min retention time. Standard calibrations for DSP were performed in triplicate in a concentration range of 0.2–400 µg/ml. The method was validated according to ICH Q2(R2) guidelines for validation of analytical procedures (EMA, 2024), for linearity (r = 0.99986), precision and accuracy. The limits of detection (LOD) and quantification (LOQ) was calculated at 0.02736 µg/ml and 0.08291 µg/ml respectively. Unknown concentrations of DSP were calculated from the linear regression of standard curves.

Apparent Permeability Coefficient: The penetration of PEAs and DSP was expressed as a normalised apparent permeability coefficient (P_{app}, cm/s) calculated using the equation: $P_{app} = \frac{Q}{t}\left(\frac{1}{A.Q_0.60}\right)$ (Begum et al., 2020; Civiale et al., 2004; Liu et al., 2014), where Q is the mass of translocated compound detected in PBS in the receptor chamber at t = 60 min, Q_0 is the initial mass of compound applied in the donor chamber and A is the area of tissue available for diffusion.

Table 1
List of CPPs used in the study with their amino acid residue sequences. To study the permeability of CPPs, fluorescein isothiocyanate (FITC) labelled peptides were used, conjugated at N terminal with a long chain (LC) to prevent degradation of FITC.

Peptide Name	Amino acid sequence (N terminal → C terminal)	Catalogue No.	Molecular weight (Da)
FITC-LC-TAT (47–57)	FITC – –LC-YG RKK RRQ RRR – NH_2	AS-27043	2063.0
FITC-LC-Antennapedia peptide/Penetratin	FITC – –LC-RQ IKI WFQ NRR MKW KK – NH_2	AS-24176	2748.9
TAT (47–57)	H – YGR KKR RQR RR – OH	AS-60023	1560.4
Penetratin	H – RQI KIW FQN RRM KWK KGG – OH	AS-64885	2362.5

2.3. Transepithelial electrical resistance measurement of corneal epithelium

Transepithelial electrical resistance (TEER) measurements were taken on the corneal discs in the *ex-vivo* permeability assays, to

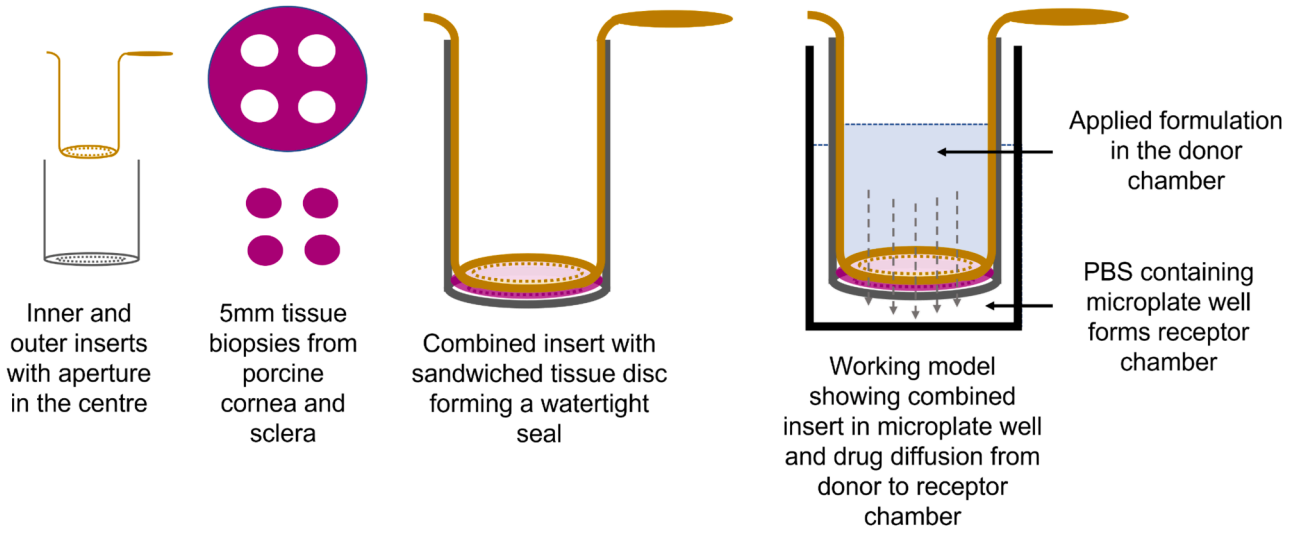

Fig. 1. Illustration of the *ex-vivo* model of permeability using porcine cornea and sclera. The inner and outer insert apertures allow diffusion of applied formulation across the membrane of cornea or sclera discs taken using a biopsy punch which were then sandwiched between the two inserts forming a watertight seal. This combined insert was then placed in a 96-well microplate well containing PBS. The formulation was applied in the donor chamber in the inner insert and its permeability assayed by measuring the concentration in the PBS in microplate well, acting as the receptor chamber.

determine the PEA toxicity on the corneal epithelial barrier integrity using a previously described method (Begum et al., 2020; Juretić et al., 2018). TEER was measured on cornea discs treated with pAc, FITC-TAT and FITC-penetratin (n = 3/group) using Millicell ERS-2 (Electrical Resistance System) volt-ohm meter (Cat no. MERS00002; Sigma-Aldrich) at RT by placing the corneal discs in a Millicell 96-well transport analysis plate (Cat no. PSHT004S5; Sigma-Aldrich) wells containing PBS and measuring the resistance values on the epithelial surface by immersing the tip of a specially designed silver/silver chloride (Ag/AgCl) electrode for 96 well plates (Cat no. MERSSTX00; Sigma-Aldrich). The resistance values were recorded from the monitor in ohms (Ω) initially at 0 min before application of compounds and finally after removal of the compounds at 60 min. PBS only wells were measured for background resistance, which was subtracted from the measured values and TEER was calculated by multiplying the recorded resistance values with the cross-sectional area of 5 mm corneal discs and expressed in Ω. cm^2. PBS treated corneal discs (n = 3) were used as controls for comparison.

2.4. Immunostaining of epithelial tight junctions

To prepare corneal discs for cryosectioning prior to immunohistochemistry, corneal discs were recovered after permeability assays and fixed in 4 % paraformaldehyde (BioReagent, ≥ 36.0 %; Cat no. 47608, Sigma-Aldrich) in PBS overnight at 4 °C followed by cryoprotection in increasing concentration of sucrose (≥99.5 %; Cat no. S9378, Sigma-Aldrich, Switzerland) solutions – 10 %, 20 % and 30 % for 8–14 h each. The tissues were then embedded in Peel-A-Way embedding moulds (Cat no. 12677736, Epredia, Fisher Scientific, USA) with optimal cutting temperature compound (OCT; Cat no. 12678646, Fisher Scientific) and frozen on dry ice to be stored at −80 °C. Frozen blocks were sectioned at 15 μm thickness using a cryostat (Brights Instruments, Huntingdon, UK) at −20 °C, and the sections were collected on SuperFrost Plus adhesion glass microscope slides (Cat no. 10149870, Fisher Scientific, Ashford, UK). The sections were allowed to settle overnight at RT before storing at −20 °C until use.

Corneal discs were immunostained for epithelial tight junction markers to detect structural damage to tight junction integrity. Frozen sections were thawed at RT for 30 min and washed 2 × 5 min in PBS, followed by permeabilisation in 0.1 % triton X-100 (Cat no. T8787, Sigma-Aldrich, USA) in PBS for 10 min. After further 2 × 5 min PBS washes at RT, sections were blocked in 0.5 % bovine serum albumin (BSA; Cat no. A3311, Sigma-Aldrich) + 0.1 % triton X-100 in PBS for 30 min at RT to prevent any non-specific binding. The tissue sections treated with pAc, FITC-TAT, FITC-penetratin, fluorescein sodium and PBS controls (n = 3/group) were then incubated with primary antibodies: ZO-1 (1:100; Rabbit Polyclonal IgG, Cat no. 40–2200, ThermoFisher) and occludin (1:100; Rabbit Polyclonal IgG, Cat no. 71–1500, ThermoFisher) separately in PBS containing 0.5 % BSA + 0.05 % tween-20 (Cat no. 663684B, VWR) and left overnight at 4 °C in a humidified chamber. The next day, sections were washed three times for 5 min in PBS and incubated with fluorescently labelled secondary antibody: Alexa Fluor Plus 594 (1:400; Donkey anti-Rabbit Polyclonal IgG; Cat no. A32754, ThermoFisher) in PBS containing 0.5 % BSA + 0.05 % tween-20 for 1 h at RT. After further washes, three times for 5 min in PBS, coverslips were mounted with Vectashield Plus antifade mounting medium containing 4′,6-diamidino-2-phenylindole (DAPI) (Cat no. H2000, Vector Laboratories, Peterborough, UK). Sections were imaged on an inverted confocal laser scanning microscope with Airyscan (LSM880; Carl Zeiss Ltd, Cambridge, UK) and two to three images were obtained using 20X objective (200X magnification) for each section with red, green and DAPI filters by an experimenter masked to the treatment conditions.

2.5. MTT assay for in-vitro cytotoxicity of PEAs

In-vitro cytotoxicity of all the PEAs was determined using MTT assay-based Cell Proliferation Kit I (Cat no. 11465007001, Sigma-Aldrich). The assays were performed according to manufacturer's instructions on human retinal pigment epithelium, ARPE-19, cell line (ATCC-CRL-2302; ATCC, Manassas, VA, USA). The cells were cultured between passages 5–7 in a 75 cm^2 tissue culture flask (Cat no. 430641, Corning) with 1:1 mixture of Dulbecco's modified eagle medium and Ham's nutrient mixture F-12 basal media (DMEM/F-12; Cat no. 31330038, ThermoFisher) containing 4-(2-Hydroxyethyl)-1-piperazine ethanesulfonic acid (HEPES) buffer, 2.5 mM L-glutamine and phenol red, and supplemented with 10 % heat-inactivated foetal bovine serum (FBS; Cat no. 10500064, ThermoFisher) and 1 % penicillin/streptomycin antibiotic mixture (5,000 U/mL; Cat no. 15070063, ThermoFisher). The cells were grown in an incubator at 37 °C in 5 % CO_2 and after reaching 80 % confluency, cells were detached using a mixture of 0.05 % (w/v) trypsin and 0.53 mM ethylene-diamine-tetra acetic acid (Trypsin-EDTA,

without phenol red; Cat no. 15400054, ThermoFisher) in sterile DPBS (Dulbecco's; Cat no. 14190094, ThermoFisher). Cells were counted and seeded at a concentration of 10^4 cells/well in 100 µl supplemented cell culture medium into tissue culture grade 96-wells flat bottom microplates (Cat no. 3596, Corning, Durham, NC, USA) and allowed to settle overnight in an incubator at 37 °C and 5 % CO_2.

The next day, media was carefully removed, and 100 µl each of the three PEAs at a range of different concentrations were added, and media only wells were used as controls. All treatments were prepared in sterile cell culture medium, and each experiment had at least 8 technical replicates for every concentration of each PEA. pAc was UV sterilised and CPPs were provided as sterile freeze-dried powders from the manufacturer. Cells were exposed to the PEAs for 24 h at 37 °C and 5 % CO_2. The PEAs were removed, and fresh culture medium was added to allow for a recovery for 48 h at 37 °C and 5 % CO_2. At this point, the media was removed and 100 µl of 0.5 mg/ml solution of MTT in sterile culture medium was added to the wells and incubated for 4 h in the dark at 37 °C, 5 % CO_2. Finally, the purple formazan crystals were solubilised with the addition of 100 µl solubilisation buffer containing 10 % sodium dodecyl sulphate (SDS) in 0.01 M hydrochloric acid (HCl). The plates were allowed to stand overnight at 37 °C, 5 % CO_2 for complete solubilisation of formazan crystals and the resulting purple solution was analysed by measuring spectrophotometric absorbance of the formazan product in the samples at 570 nm in a microplate reader (BMG Clairostar, Ortenberg, Germany). The experiment was repeated three times (n = 3), and half maximal inhibitory concentration (IC_{50}) values were calculated for each PEA from the non-linear sigmoidal fits of the dose–response curves.

2.6. Statistical analysis

The data were analysed in OriginPro, Version 2021b SR1 (OriginLab Corporation, Northampton, MA, USA). All values are presented as mean ± standard error of mean (SEM). P_{app} data was tested for normality using Shapiro-Wilk test and accordingly parametric or non-parametric tests were used for further analysis. For a parametrically distributed data, one-way ANOVA with post-hoc Bonferroni's multi comparisons test was used, while Kruskal-Wallis ANOVA with post-hoc Dunn's pairwise comparisons test was used for non-parametrically distributed data. A p value < 0.05 was set as the threshold for statistical significance.

3. Results

3.1. All three PEAs increased corneal permeability of DSP ex-vivo

pAc, FITC-TAT, and FITC-penetratin all showed significantly higher permeabilities compared to fluorescein sodium controls across both cornea and sclera in the permeability assays (Table 2 and Fig. 2(a)). Among the three PEAs, FITC-penetratin had the highest corneal permeability, up to 5 times higher ($p < 0.0001$) than the corneal P_{app} of fluorescein after 60 min. All PEAs showed up to 2-fold higher ($p < 0.05$) permeabilities across the sclera compared to fluorescein controls. However, all the PEAs showed similar permeabilities amongst them across the sclera. Though pAc and fluorescein's scleral P_{app} values were almost double as compared to their corneal P_{app} values, CPPs showed slightly lower scleral permeabilities compared to their corneal permeabilities.

All three PEAs – pAc, TAT, and penetratin, significantly increased the corneal permeability of DSP in formulations in permeability assays (Table 3 and Fig. 2(b)). TAT exhibited the most statistically significant enhancement of DSP corneal uptake after 60 min at 6-fold ($p = 0.0377$), pAc increased the DSP corneal permeability by 5-fold ($p = 0.0130$), whereas penetratin showed the highest increase in mean value of DSP corneal permeabilities by up to 7-fold higher ($p = 0.9540$). However, there was no enhancement in scleral permeability of DSP with any of the PEAs. DSP's scleral P_{app} with pAc and penetratin at 60 min was much lower – almost half compared to the scleral P_{app} of DSP by itself, and its scleral P_{app} with TAT remained similar to its scleral P_{app} by itself. The scleral permeability of DSP itself was upwards of 10 times higher than its permeability in the cornea. With pAc and penetratin, DSP's scleral permeability was almost similar compared to the permeability in cornea, whereas its scleral permeability with TAT was almost double than the corneal permeability.

3.2. Peas cause no irreversible damage to the barrier integrity of corneal epithelium or epithelial tight junctions

TEER measurements on the corneal discs treated with PEAs and PBS controls showed no significant differences in TEER over 60 min as depicted in Fig. 3. In fact, control discs exhibited the maximum drop in TEER values at 5.90 ± 2.91 % from 181.62 ± 22.52 Ω.cm^2 at 0 min to 172.1 ± 25.82 Ω.cm^2 at 60 min, compared to drop in pAc tissues at 2.33 ± 0.58 % from 75.07 ± 4.48 Ω.cm^2 at 0 min to 73.38 ± 4.8 Ω.cm^2 at 60 min, in FITC-TAT at 2.66 ± 0.36 % from 79.32 ± 8.63 Ω.cm^2 at 0 min to 77.24 ± 8.56 Ω.cm^2 at 60 min, and that of FITC-penetratin at 4.61 ± 1.59 % from 93.16 ± 4.29 Ω.cm^2 at 0 min to 88.74 ± 2.55 Ω.cm^2 at 60 min. Immunostaining in the corneal sections with ZO-1 and occludin showed characteristic staining of tight junctions in the apical cell layers of corneal epithelium with all PEAs, and identical to PBS treated controls, as shown in different panels in Fig. 4. There was no breakdown of surface cellular layers at any point confirming that the integrity of the corneal barrier is preserved.

3.3. PEAs exhibit safe levels of in-vitro tolerance in ARPE-19 cells at clinically relevant concentrations

All the three PEAs were tolerated well *in-vitro* in ARPE-19 cell toxicity assays, as evidenced in the dose response curves in Fig. 5. IC_{50} values as calculated from these curves for pAc was 64.79 mM, for CPPs TAT and penetratin it was 1335.45 µM and 87.26 µM respectively, which was much higher than we used *ex-vivo* in all cases except penetratin.

Table 2
P_{app} (Mean ± SEM) values for all PEAs and fluorescein from permeability assays, and ratios of means as a comparative analysis of permeability of PEAs to that of fluorescein across cornea (n = 12/group) and sclera (n = 9/group). The statistical significance of the results is demonstrated by p values.

Compound	Cornea (n = 12/group)			Sclera (n = 9/group)		
	P_{app} (Mean ± SEM) X 10^{-4} cm/s	Mean ratio to Fluorescein Control	p value (compared with fluorescein)	P_{app} (Mean ± SEM) X 10^{-4} cm/s	Mean ratio to Fluorescein Control	p value (compared with fluorescein)
pAc (2.21 mg/ml; 19.36 mM)	1.09 ± 0.18	2.69	<0.001	1.90 ± 0.44	2.07	0.0195
FITC-TAT (100 µM)	1.72 ± 0.13	4.24	<0.0001	1.68 ± 0.28	1.84	0.01726
FITC-penetratin (100 µM)	2.01 ± 0.06	4.94	<0.0001	1.84 ± 0.26	2.00	0.0035
Fluorescein (100 µM)	0.41 ± 0.04			0.92 ± 0.07		

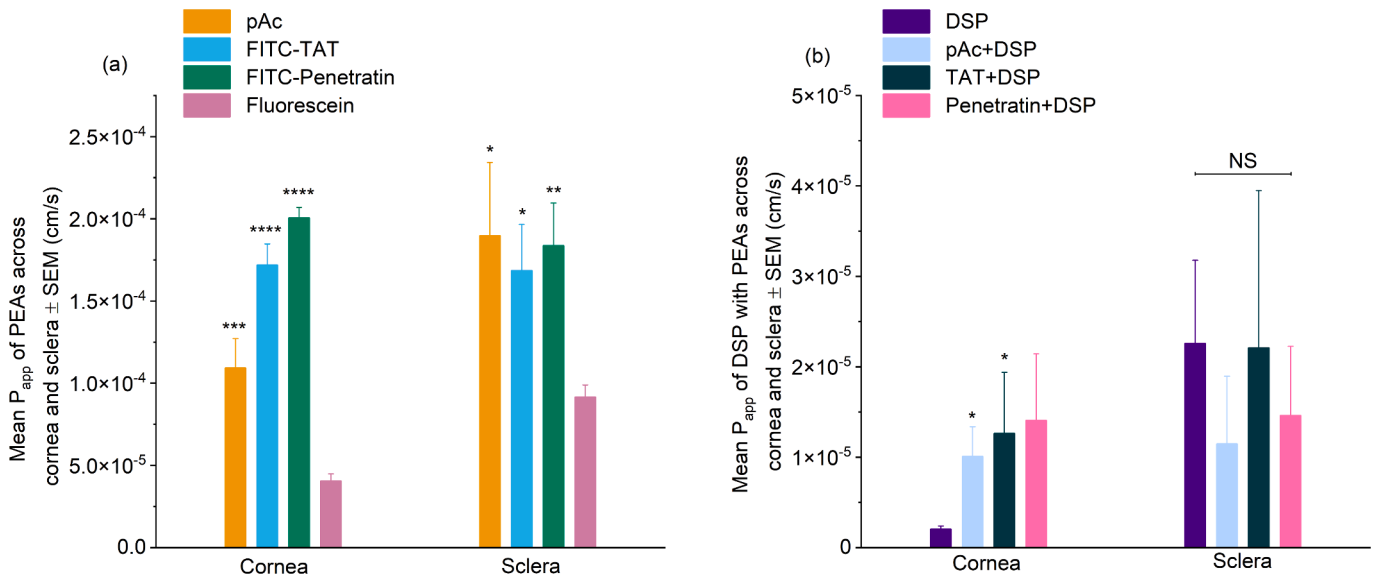

Fig. 2. Mean ± SEM P_{app} plots of PEAs (a) and DSP in formulation with PEAs (b) in cornea (n = 12/group) and sclera (n = 9/group) from permeability assays at 60 min. (a) All three PEAs show higher permeabilities across both cornea and sclera compared with fluorescein controls. In cornea and sclera respectively: pAc ≈ 2.7X (***p < 0.001) and ≈ 2.1X (*p = 0.0195); FITC-TAT ≈ 4.2X (****p < 0.0001) and ≈ 1.8X (*p = 0.0173); FITC-penetratin ≈ 4.9X (****p < 0.0001) and ≈ 2X (**p = 0.0035). (b) All PEAs increase corneal uptake of DSP: pAc ≈ 4.9X (*p = 0.0130); TAT ≈ 6.2X (*p = 0.0377); Penetratin ≈ 6.9X (p = 0.9540). However, there is no enhancement observed in the uptake of DSP across sclera with any of the PEAs. NS = not significant.

Table 3
Calculated P_{app} values (Mean ± SEM) of DSP alone and in formulations with different PEAs showing the comparative uptake across cornea (n = 12/group) and sclera (n = 9/group) with all PEAs, as observed by the ratios of means of DSP P_{app} with PEAs to the DSP P_{app} by itself, and their statistical significance (p values) in enhancing DSP uptake.

Formulation	Cornea (n = 12/group)			Sclera (n = 9/group)		
	P_{app} (Mean ± SEM) X 10^{-5} cm/s	Mean ratio to DSP only	p value (compared with DSP)	P_{app} (Mean ± SEM) X 10^{-5} cm/s	Mean ratio to DSP only	p value (compared with DSP)
DSP (10 mg/ml)	0.20 ± 0.04			2.26 ± 0.92		
pAc (2.21 mg/ml) + DSP	1.01 ± 0.33	4.93	0.0130	1.15 ± 0.75	0.51	0.1451
TAT (100 μM) + DSP	1.26 ± 0.68	6.18	0.0377	2.21 ± 1.74	0.98	0.0703
Penetratin (100 μM) + DSP	1.41 ± 0.74	6.88	0.9540	1.46 ± 0.77	0.65	0.2697

4. Discussion

We aimed to increase DSP bioavailability in the posterior segment of the eye after topical administration using PEAs as a delivery agent. We showed that all three PEAs increased corneal permeability of DSP by several fold over control formulations. We also showed that none of the PEAs caused damage to the barrier integrity of the cornea by immunohistochemistry for tight junction proteins, including ZO-1 and occludin and PEAs had no effect on ARPE-19 cell viability at clinically relevant concentrations. These results suggest that PEAs increase DSP corneal permeability after topical application and may be used clinically to increase the bioavailability of DSP for the treatment of inflammatory conditions in the eye.

Dexamethasone is a corticosteroid used primarily in eye drop formulations to treat inflammation in the eye, particularly after cataract surgery (Karasu et al., 2022). However, it is practically insoluble in aqueous systems, which limits its use for topical ophthalmic administration (Shen et al., 2021). Dexamethasone's hydrophilic prodrug – the sodium-phosphate ester, DSP, is poorly permeable and hence efforts to overcome this limitation have been explored to allow local drug administration in posterior segment disease. For example, intravitreal implants of dexamethasone (Ozurdex) have been developed and used to treat diabetic macular oedema and macular oedema secondary to retinal vein occlusion and posterior uveitis, however, this requires intravitreal implantation and hence is an expensive treatment option, with a risk of complications that may worsen patients' vision (Massa et al., 2019).

Intracanalicular implants have also been tested for sustained release of dexamethasone to the ocular surface (Lee and Blair, 2020; Walters et al., 2015). In clinical trials, one-off intracameral delivery of dexamethasone was preferred by patients undergoing cataract surgery and proved to be effective at reducing pain, inflammation, and thus improved visual acuity (Hovanesian and Donnenfeld, 2022). However, topical delivery of dexamethasone remains the most versatile, cheapest, and patient-friendly option for long-term treatment. Recent efforts in this regard have resulted in development of cyclodextrin – dexamethasone inclusion complexes micro-suspension which has been validated to achieve a therapeutic bioavailability of dexamethasone to the posterior segment by topical eye-drop instillation in an *in-vivo* animal model (Johannsdottir et al., 2018), showed significant improvement in patients with diabetic macular oedema in a phase II randomised controlled trial (RCT) (Stefansson et al., 2023), and is currently in phase III clinical trial ("Oculis | Oculis Announces First Patient First Visit in Phase 3 OPTIMIZE-2 Trial of OCS-01 for the Treatment of Inflammation and Pain Following Cataract Surgery," n.d.).

To measure the permeability of our PEAs and DSP formulations *ex-vivo* across cornea and sclera, we employed a novel diffusion model using porcine eye tissues owing to easy availability as a meat industry excess and overwhelming anatomical similarities with human eye

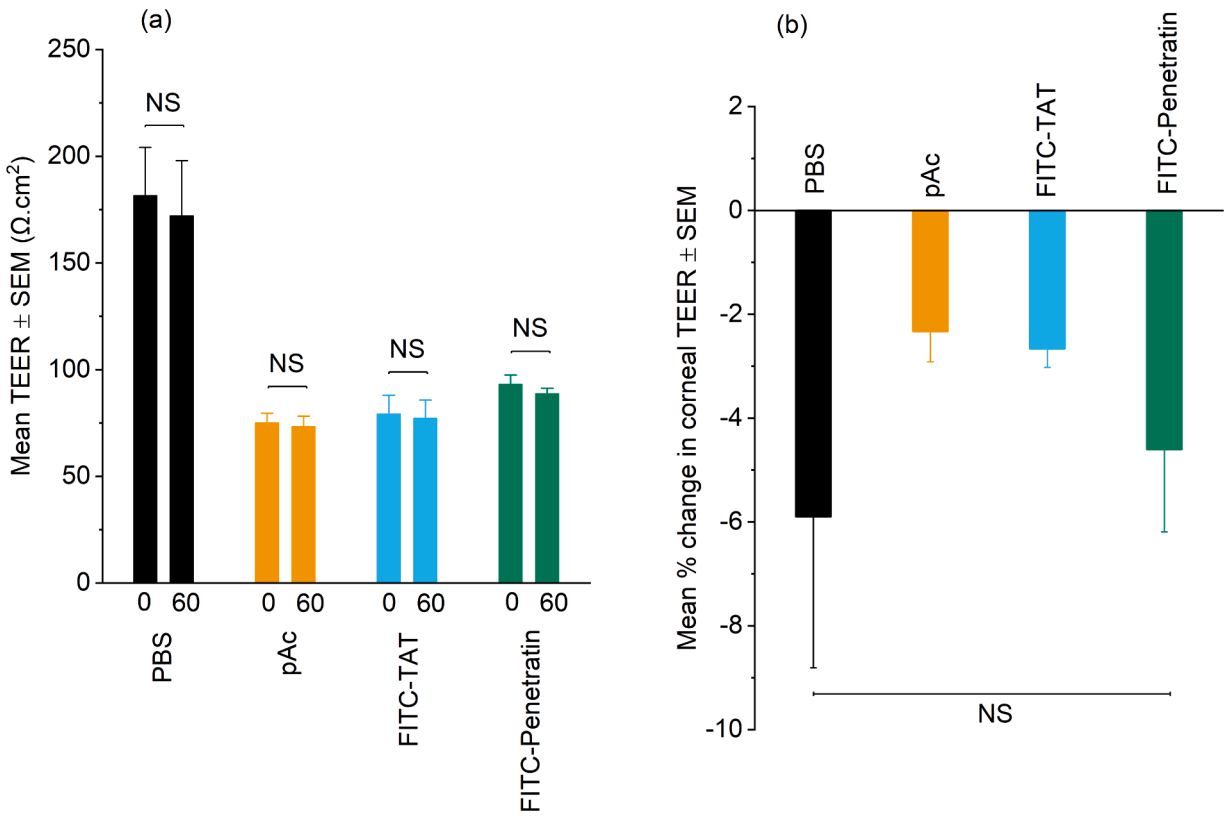

Fig. 3. Plots representing (a) TEER values and (b) percentage change in TEER (mean ± SEM; n = 3/PEA) over 60 min of application of PEAs on corneal surfaces in assays. The drop in TEER values for all PEAs is lower than that of PBS controls. NS = not significant.

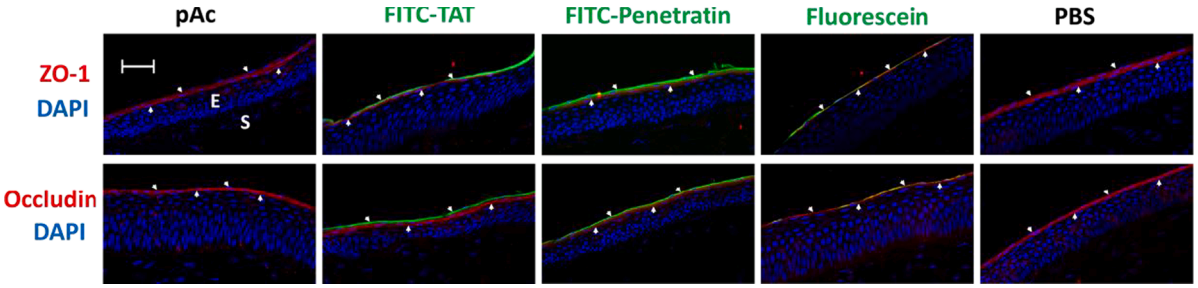

Fig. 4. Confocal micrographs of cross sections of corneas at 200X magnification stained with ZO-1 and occludin after permeability assays showing corneal epithelium (E) and stroma (S). Tight junctions between the superficial stratified squamous epithelial cells with flat nuclei are stained in red for ZO-1 and occludin in the 2–3 apical layers of corneal epithelium as shown by white arrows. No staining was observed in either wing or basal cell layers in the epithelium. FITC conjugated CPPs and fluorescein also show a green-fluorescent layer on the top indicating surface retention of PEAs, however no such fluorescence was seen in deeper layers within epithelium or further down in stroma and endothelium. DAPI stained nuclei in blue; scale bar 50 μm; n = 3 sections per PEA.

compared to other non-primate mammals. Porcine corneas are only slightly thicker than human corneas (Blanch et al., 2012; Faber et al., 2008), and the epithelium also has 1–2 extra cell layers (Ehlers, 1970) whereas porcine sclera is double in thickness to human sclera but has exactly similar composition and histology (Nicoli et al., 2009). Normally, drugs applied to the ocular surface are instantly cleared, showing a 100 % surface elimination within a maximum 15–20 min (Balla et al., 2022), thus limiting its precorneal residence time and bioavailability. Our rapid assay miniaturised model of permeability is favourable for shorter durations. The model only uses a 5 mm biopsy of the tissue instead of whole cornea or sclera (Begum et al., 2021, 2020), thus reducing the need for tissue and multiplexing its use by maximising the throughput in a 96-well microplate subscribing to the 3Rs principles of animal research (Graham and Prescott, 2015; Sneddon et al., 2017) and the FDA modernisation act 2.0 (Stewart et al., 2023). PEAs were transported across both cornea and sclera at a rate much faster than fluorescein controls, with P_{app} values up to 5 times higher in cornea and 2X in sclera, however there were no differences between the corneal and scleral permeabilities of PEAs except for pAc.

Transport of CPPs across lipophilic and negatively charged corneal epithelium would necessarily be through transcellular means following either energy dependent endocytic pathways or passive direct translocation or a combination of both depending upon the concentration (Duchardt et al., 2007; Lindgren et al., 2004; Lundin et al., 2008; Richard et al., 2003), aided by their cationic and amphipathic nature, while hydrophilic stroma and endothelium should ideally offer no hinderance. A negatively charged and hydrophilic fluorescein sodium dye would be blocked transcellularly and only show low paracellular transport across the cornea due to its small molecular size, as is consistent with our results. However, the sclera does not have distinct cell layers but instead is an aqueous matrix of collagen fibre bundles with embedded fibroblasts and negatively charged proteoglycans, and

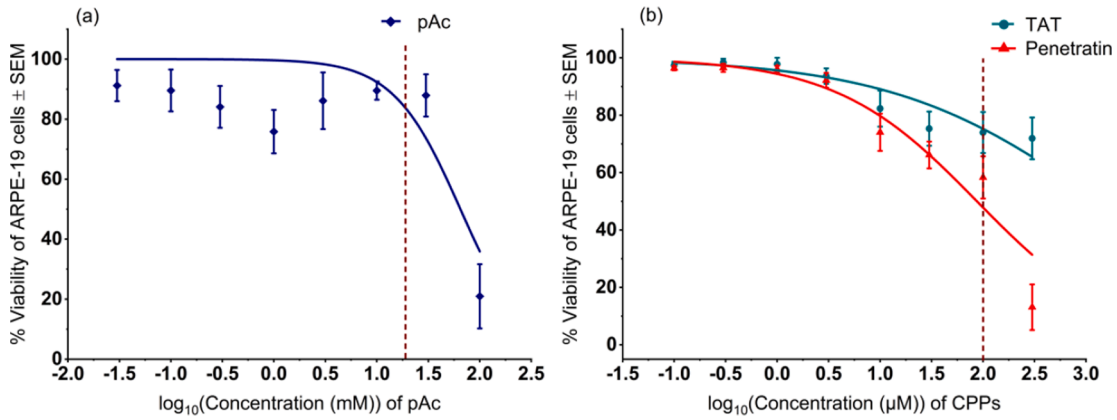

Fig. 5. Dose response curves of (a) pAc and (b) CPPs TAT and penetratin showing percentage viability of ARPE-19 cells (Mean ± SEM; n = 3/PEA) against $\log_{10}$ concentration range of PEAs, from which IC_{50} values were calculated to evaluate their tolerance *in-vitro*. Dotted lines denote the concentrations used for *ex-vivo* permeability measurement.

the permeability would depend on molecular weight and hydrodynamic radius of PEAs making their way through this matrix (Ambati et al., 2000; Trier, 2005; Wen et al., 2013), supporting the higher P_{app} of fluorescein across sclera compared to cornea whereas CPPs having a larger molecular radius show similar P_{app} in cornea and sclera. However, an amphiphilic pAc with a much smaller size would not face any resistance across sclera.

Permeability of DSP across the cornea was enhanced more than 6 times in combination with PEAs. DSP being a hydrophilic ester of dexamethasone, with a water/octanol partition coefficient (log P) value of 0.54 as opposed to 2.12 for dexamethasone, showed very low P_{app} values across cornea by itself, as it is obstructed by the corneal epithelium and paracellular transport is limited due to molecular size, but, hydrolysis of some of DSP into dexamethasone alcohol by phosphatase enzymes on corneal surface would result in transcellular transport of lipophilic dexamethasone, which would then be limited by the corneal stroma (Baeyens et al., 1997; Civiale et al., 2004; Weijtens et al., 2002). Therefore, there is also a difficulty in simultaneously estimating the concentrations of DSP and dexamethasone in the receptor chamber, depending upon the rate of hydrolysis, which needs to be addressed in future pharmacokinetic studies.

However, a very high aqueous solubility of DSP would ideally cancel some of the hydrophilic limitations on permeability, as suspension particles are cleared much more quickly from the ocular surface (Schoenwald and Ward, 1978). pAc would ideally conjugate with DSP through the formation of an acyl hydrazone following dynamic covalent chemistry and DSP release can be triggered by hydrolysis of the acyl hydrazone at an acidic pH in endosomes in case of endocytic uptake (Priegue et al., 2018; Ulrich, 2019). It is worth noting here that the CPPs are not covalently conjugated to DSP rather simply mixed to complex with DSP by non-covalent interactions and it has been shown that CPPs are highly effective in binding to a variety of cargoes non-covalently and transporting them across cells without hampering the uptake efficacy of complexes by avoiding any chemical modification of the drug which preserves its pharmacological activity and does not cause unintended clearance, and this is also sometimes the preferred mode of combining cargoes to CPPs as it broadens the scope for their use (Hu et al., 2009; Keller et al., 2013).

The non-corneal route of drug transport to the posterior segment through conjunctiva-sclera-choroid has been suggested to contribute a major chunk of bioavailability in retina and other tissues, especially for hydrophilic drugs (Ahmed and Patton, 1987; Hughes et al., 2005), thus it was important to test for scleral permeability alongside cornea. As was evident from our results, we observed no enhancement in DSP transport across sclera with any of the PEAs, and all of them showed lower P_{app} of DSP compared to DSP itself – up to half its original value. At the same time, DSP on its own had a 10 times higher permeability across sclera compared to cornea because an aqueous sclera does not limit the transport of hydrophilic molecules. Moreover, it can be deduced that PEAs likely inhibited DSP penetration across sclera due to the formation of a complex of size much bigger than the radius of DSP, following that transport across sclera is dependent on the size of the molecules as a small molecule DSP would travel much faster across the scleral matrix than a larger PEA-DSP complex. It is important to note that in this study we have only used sclera *ex-vivo* after removing the vascular layers of conjunctiva and choroid, however the non-corneal absorption is limited by clearance via lymphatics and vasculature of conjunctiva and choroid, and further blocked by the tight retinal pigment epithelium (RPE) and Bruch's membrane (Ahmed and Patton, 1987; Ranta et al., 2010; Robinson et al., 2006). Therefore, future studies should use a combined barrier system of conjunctiva-sclera-choroid.

Finally, TEER and immunostaining showed that none of the PEAs caused any damage or structural toxicity to the corneal barrier integrity, as TEER is a very sensitive electrophysiological indicator of barrier function of corneal epithelium (Kusano et al., 2010), while ZO-1 and occludin are cytoplasmic and transmembrane proteins respectively that constitute tight junctions between adjacent cells in the superficial layers of corneal epithelium and protect the barrier by regulating and restricting the paracellular transport of any foreign molecule (Ban et al., 2003; Contreras-Ruiz et al., 2012; Sugrue and Zieske, 1997). CPPs are often feared for inducing toxicity by causing cell membrane perturbations and leakage by pore formation (Eiríksdóttir et al., 2010; El-Andaloussi et al., 2007). However, our results showed no disruption to the structure of cell membranes of superficial epithelial cells by PEAs, and therefore, the cellular resistance was maintained in the apical layer of corneal epithelium. This was also corroborated by the IC_{50} values obtained from MTT assays on ARPE-19 cell line *in-vitro,* and any future *in-vivo* work could use a range of concentrations of PEAs below the obtained values. However, since the CPPs used in MTT assays were non-labelled, as opposed to FITC labelled ones in penetration assays, they might show different toxicities in either case, as fluorophore labelling can also affect the cytotoxicity of CPPs by modulating the net charge and hydrophobicity of the CPP (Birch et al., 2017).

5. Conclusion

The PEAs tested, including penetratin, TAT, and pAc, are all capable of improving the corneal permeability of DSP by several fold and hence DSP bioavailability in the posterior segment of the eye should be increased significantly after topical application. This would help reduce frequent intraocular injections and a higher treatment compliance by potentially allowing self-administered treatments for posterior segment

degenerative and inflammatory conditions. Though even after corneal penetration, there are multiple other physiological dynamic barriers to overcome before reaching the retina, the increased corneal permeability of hydrophilic drugs combined with the bioavailability from non-corneal transport would significantly increase the total drug penetration in the posterior segment. We have presented a more versatile alternative platform for topical ocular drug delivery to the retina using simple mixing of PEAs with drugs without the need of chemical modifications as compared to the more complicated synthesis and surface modification of nanoparticulate drug delivery systems. At the same time, it is evident from our work that these PEAs do not induce *in-vitro* cytotoxicity and do not cause any damage to the defensive barrier property of cornea *ex-vivo,* which is a common occurrence with nanoparticles. Further studies would be required to determine the therapeutic efficacy, safety, and pharmacokinetics-pharmacodynamics (PK/PD) of the formulations *in-vivo* in animal models. This proof of concept can then be used to deliver similar small molecule drugs and even macromolecular biologics to the posterior segment that can currently only be delivered through invasive intraocular administration.

CRediT authorship contribution statement

Abhinav Thareja: Writing – original draft, Visualization, Validation, Resources, Methodology, Investigation, Formal analysis, Data curation. **Thomas Leigh:** Validation, Methodology, Investigation, Formal analysis, Data curation. **Jenni J. Hakkarainen:** Writing – review & editing, Supervision, Funding acquisition. **Helen Hughes:** Writing – review & editing, Supervision, Funding acquisition. **Carmen Alvarez-Lorenzo:** Writing – review & editing, Supervision, Funding acquisition. **Francisco Fernandez-Trillo:** Writing – review & editing, Supervision, Conceptualization. **Richard J. Blanch:** Writing – review & editing, Supervision, Conceptualization. **Zubair Ahmed:** Writing – review & editing, Supervision, Project administration, Funding acquisition, Conceptualization.

Declaration of competing interest

The authors declare that they have no known competing financial interests or personal relationships that could have appeared to influence the work reported in this paper.

Data availability

Data will be made available on request.

Acknowledgements

This work was supported by the European Union's Horizon 2020 research and innovation programme under the Marie-Skłodowska-Curie Actions grant agreement N° 813440 (ORBITAL– Ocular Research by Integrated Training And Learning). Francisco Fernandez-Trillo thanks the University of Birmingham for the John Evans Fellowship, and the Spanish Ministerio de Educación, Cultura y Deporte for a Beatriz Galindo Award [BG20/00213]. Thomas Leigh acknowledges financial support from the Engineering and Physical Sciences Research Council (EPSRC) through a studentship from the Centre for Doctoral Training in Physical Sciences for Health (EP/L016346/1). Francisco Fernandez-Trillo and Richard Blanch thank the University of Birmingham and the Wellcome Trust for financial support. The funders had no involvement in study design; in the collection, analysis, and interpretation of data; in the writing of the report; and in the decision to submit the article for publication.

References

Abadia, B., Calvo, P., Ferreras, A., Bartol, F., Verdes, G., Pablo, L., 2016. Clinical applications of dexamethasone for aged eyes. Drugs Aging 33, 639–646. https://doi.org/10.1007/s40266-016-0392-z.

Ahmed, I., Patton, T.F., 1987. Disposition of timolol and inulin in the rabbit eye following corneal versus non-corneal absorption. Int. J. Pharm. 38, 9–21. https://doi.org/10.1016/0378-5173(87)90092-5.

Ambati, J., Canakis, C.S., Miller, J.W., Gragoudas, E.S., Edwards, A., Weissgold, D.J., Kim, I., Delori, F.C., Adamis, A.P., 2000. Diffusion of high molecular weight compounds through sclera. Investig. Ophthalmol. vis. Sci. 41, 1181–1185.

Baeyens, V., Varesio, E., Veuthey, J.L., Gurny, R., 1997. Determination of dexamethasone in tears by capillary electrophoresis. J. Chromatogr. B Biomed. Appl. 692, 222–226. https://doi.org/10.1016/S0378-4347(96)00494-X.

Balguri, S.P., Adelli, G.R., Majumdar, S., 2016. Topical ophthalmic lipid nanoparticle formulations (SLN, NLC) of indomethacin for delivery to the posterior segment ocular tissues. Eur. J. Pharm. Biopharm. 109, 224–235. https://doi.org/10.1016/j.ejpb.2016.10.015.

Balla, A., Ruponen, M., Valtari, A., Toropainen, E., Tuomainen, M., Alvarez-Lorenzo, C., del Amo, E.M., Urtti, A., Vellonen, K.S., 2022. Understanding dexamethasone kinetics in the rabbit tear fluid: Drug release and clearance from solution, suspension and hydrogel formulations. Eur. J. Pharm. Biopharm. 172, 53–60. https://doi.org/10.1016/j.ejpb.2022.01.005.

Ban, Y., Dota, A., Cooper, L.J., Fullwood, N.J., Nakamura, T., Tsuzuki, M., Mochida, C., Kinoshita, S., 2003. Tight junction-related protein expression and distribution in human corneal epithelium. Exp. Eye Res. 76, 663–669. https://doi.org/10.1016/S0014-4835(03)00054-X.

Bechara, C., Sagan, S., 2013. Cell-penetrating peptides: 20 years later, where do we stand? FEBS Lett. https://doi.org/10.1016/j.febslet.2013.04.031.

Begum, G., Leigh, T., Courtie, E., Moakes, R., Butt, G., Ahmed, Z., Rauz, S., Logan, A., Blanch, R.J., 2020. Rapid assessment of ocular drug delivery in a novel ex vivo corneal model. Sci. Rep. 10, 11754. https://doi.org/10.1038/s41598-020-68254-1.

Begum, G., Leigh, T., Stanley, D., Logan, A., Blanch, R.J., 2021. Determining the effect of ocular chemical injuries on topical drug delivery. Drug Deliv. 28, 2044–2050. https://doi.org/10.1080/10717544.2021.1979124.

Birch, D., Christensen, M.V., Staerk, D., Franzyk, H., Nielsen, H.M., 2017. Fluorophore labeling of a cell-penetrating peptide induces differential effects on its cellular distribution and affects cell viability. Biochim. Biophys. Acta - Biomembr. 1859, 2483–2494. https://doi.org/10.1016/J.BBAMEM.2017.09.015.

Blanch, R.J., Ahmed, Z., Berry, M., Scott, R.A.H., Logan, A., 2012. Animal models of retinal injury. Invest. Ophthalmol. vis. Sci. 53, 2913–2920. https://doi.org/10.1167/iovs.11-8564.

Ciulla, T.A., Walker, J.D., Fong, D.S., Criswell, M.H., 2004. Corticosteroids in posterior segment disease: An update on new delivery systems and new indications. Curr. Opin. Ophthalmol. 15, 211–220. https://doi.org/10.1097/01.icu.0000120711.35941.76.

Civiale, C., Bucaria, F., Piazza, S., Peri, O., Miano, F., Enea, V., 2004. Ocular permeability screening of dexamethasone esters through combined cellular and tissue systems. J. Ocul. Pharmacol. Ther. 20, 75–84. https://doi.org/10.1089/108076804772745482.

Contreras-Ruiz, L., Schulze, U., García-Posadas, L., Arranz-Valsero, I., López-García, A., Paulsen, F., Diebold, Y., 2012. Structural and functional alteration of corneal epithelial barrier under inflammatory conditions. Curr. Eye Res. 37, 971–981. https://doi.org/10.3109/02713683.2012.700756.

Desai, N., 2012. Challenges in development of nanoparticle-based therapeutics. AAPS J. 14, 282–295. https://doi.org/10.1208/s12248-012-9339-4.

Duchardt, F., Fotin-Mleczek, M., Schwarz, H., Fischer, R., Brock, R., 2007. A comprehensive model for the cellular uptake of cationic cell-penetrating peptides. Traffic 8, 848–866. https://doi.org/10.1111/j.1600-0854.2007.00572.x.

Dugel, P.U., Bandello, F., Loewenstein, A., 2015. Dexamethasone intravitreal implant in the treatment of diabetic macular edema. Clin. Ophthalmol. 9, 1321–1335. https://doi.org/10.2147/OPTH.S79948.

Ehlers, N., 1970. Morphology and histochemistry of the corneal epithelium of mammals. Cells Tissues Organs 75, 161–198. https://doi.org/10.1159/000143448.

Ehlken, C., Ziemssen, F., Eter, N., Lanzl, I., Kaymak, H., Lommatzsch, A., Schuster, A.K., 2020. Systematic review: non-adherence and non-persistence in intravitreal treatment. Graefe's Arch. Clin. Exp. Ophthalmol. 258, 2077–2090. https://doi.org/10.1007/s00417-020-04798-2.

Eiríksdóttir, E., Konate, K., Langel, Ü., Divita, G., Deshayes, S., 2010. Secondary structure of cell-penetrating peptides controls membrane interaction and insertion. Biochim. Biophys. Acta - Biomembr. 1798, 1119–1128. https://doi.org/10.1016/j.bbamem.2010.03.005.

El-Andaloussi, S., Järver, P., Johansson, H.J., Langel, Ü., 2007. Cargo-dependent cytotoxicity and delivery efficacy of cell-penetrating peptides: A comparative study. Biochem. J. 407, 285–292. https://doi.org/10.1042/BJ20070507.

Ema, 2024. ICH Q2(R2) Validation of analytical procedures - Scientific guideline | European Medicines Agency [WWW Document]. accessed 3.24.23. https://www.ema.europa.eu/en/ich-q2r2-validation-analytical-procedures-scientific-guideline.

Faber, C., Scherfig, E., Prause, J.U., Sørensen, K.E., 2008. Corneal thickness in pigs measured by ultrasound pachymetry in vivo. Scand. J. Lab. Anim. Sci. 35, 39–43. https://doi.org/10.23675/sjlas.v35i1.139.

Fernandez Trillo, F., Blanch, R.J., 2023. Polymers for enhancing the ocular penetration of therapeutic agents. Eur. Pat. Off. EP23383289.8.

Gaballa, S.A., Kompella, U.B., Elgarhy, O., Alqahtani, A.M., Pierscionek, B., Alany, R.G., Abdelkader, H., 2021. Corticosteroids in ophthalmology: drug delivery innovations,

pharmacology, clinical applications, and future perspectives. Drug Deliv. Transl. Res. 11, 866–893. https://doi.org/10.1007/s13346-020-00843-z.
Good, T.J., Kimura, A.E., Mandava, N., Kahook, M.Y., 2011. Sustained elevation of intraocular pressure after intravitreal injections of anti-VEGF agents. Br. J. Ophthalmol. 95, 1111–1114. https://doi.org/10.1136/bjo.2010.180729.
Graham, M.L., Prescott, M.J., 2015. The multifactorial role of the 3Rs in shifting the harm-benefit analysis in animal models of disease. Eur. J. Pharmacol. 759, 19–29. https://doi.org/10.1016/j.ejphar.2015.03.040.
Haller, J.A., Bandello, F., Belfort, R., Blumenkranz, M.S., Gillies, M., Heier, J., Loewenstein, A., Yoon, Y.H., Jacques, M.L., Jiao, J., Li, X.Y., Whitcup, S.M., 2010. Randomized, Sham-Controlled Trial of Dexamethasone Intravitreal Implant in Patients with Macular Edema Due to Retinal Vein Occlusion. Ophthalmology 117, 1134–1146.e3. https://doi.org/10.1016/j.ophtha.2010.03.032.
Hovanesian, J.A., Donnenfeld, E.D., 2022. Intracameral dexamethasone 9% vs prednisolone acetate 1% in controlling postoperative pain and inflammation in patients undergoing cataract surgery. J. Cataract Refract. Surg. 48, 906–911. https://doi.org/10.1097/j.jcrs.0000000000000887.
Hu, J.W., Liu, B.R., Wu, C.Y., Lu, S.W., Lee, H.J., 2009. Protein transport in human cells mediated by covalently and noncovalently conjugated arginine-rich intracellular delivery peptides. Peptides 30, 1669–1678. https://doi.org/10.1016/j.peptides.2009.06.006.
Hughes, P.M., Olejnik, O., Chang-Lin, J.E., Wilson, C.G., 2005. Topical and systemic drug delivery to the posterior segments. Adv. Drug Deliv. Rev. 57, 2010–2032. https://doi.org/10.1016/j.addr.2005.09.004.
Johannsdottir, S., Jansook, P., Stefansson, E., Kristinsdottir, I.M., Fulop, Z., Asgrimsdottir, G.M., Thorsteindsottir, M., Eiriksson, F.F., Loftsson, T., 2018. Topical drug delivery to the posterior segment of the eye: Dexamethasone concentrations in various eye tissues after topical administration for up to 15 days to rabbits. J. Drug Deliv. Sci. Technol. 45, 449–454. https://doi.org/10.1016/j.jddst.2018.04.007.
Juretić, M., Cetina-Čižmek, B., Filipović-Grčić, J., Hafner, A., Lovrić, J., Pepić, I., 2018. Biopharmaceutical evaluation of surface active ophthalmic excipients using in vitro and ex vivo corneal models. Eur. J. Pharm. Sci. 120, 133–141. https://doi.org/10.1016/j.ejps.2018.04.032.
Karabag, R.Y., Parlak, M., Cetin, G., Yaman, A., Osman Saatci, A., 2015. Retinal tears and rhegmatogenous retinal detachment after intravitreal injections: its prevalence and case reports. Digit. J. Ophthalmol. DJO 21, 8–10. https://doi.org/10.5693/djo.01.2014.07.001.
Karasu, B., Kesim, E., Kaskal, M., Celebi, A.R.C., 2022. Efficacy of topical dexamethasone eye drops in preventing ocular inflammation and cystoid macular edema following uncomplicated cataract surgery with or without injection of a single dose perioperative subtenon triamcinolone acetonide. Cutan. Ocul. Toxicol. 41, 310–317. https://doi.org/10.1080/15569527.2022.2136193.
Kaur, I.P., Smitha, R., 2002. Penetration enhancers and ocular bioadhesives: Two new avenues for ophthalmic drug delivery. Drug Dev. Ind. Pharm. 28, 353–369. https://doi.org/10.1081/DDC-120002997.
Keller, A.A., Mussbach, F., Breitling, R., Hemmerich, P., Schaefer, B., Lorkowski, S., Reissmann, S., 2013. Relationships between cargo, cell penetrating peptides and cell type for uptake of non-covalent complexes into live cells. Pharmaceuticals 6, 184–203. https://doi.org/10.3390/ph6020184.
Kusano, M., Uematsu, M., Kumagami, T., Sasaki, H., Kitaoka, T., 2010. Evaluation of acute corneal barrier change induced by topically applied preservatives using corneal transepithelial electric resistance in vivo. Cornea 29, 80–85. https://doi.org/10.1097/ICO.0b013e3181a3c3e6.
Lai, S., Wei, Y., Wu, Q., Zhou, K., Liu, T., Zhang, Y., Jiang, N., Xiao, W., Chen, J., Liu, Q., Yu, Y., 2019. Liposomes for effective drug delivery to the ocular posterior chamber. J. Nanobiotechnology 17, 64. https://doi.org/10.1186/s12951-019-0498-7.
Lee, A., Blair, H.A., 2020. Dexamethasone Intracanalicular Insert: A Review in Treating Post-Surgical Ocular Pain and Inflammation. Drugs 80, 1101–1108. https://doi.org/10.1007/s40265-020-01344-6.
Leigh, T., Fernandez-Trillo, P., 2020. Helical polymers for biological and medical applications. Nat. Rev. Chem. 4, 291–310. https://doi.org/10.1038/s41570-020-0180-5.
Lindgren, M.E., Hällbrink, M.M., Elmquist, A.M., Langel, Ü., 2004. Passage of cell-penetrating peptides across a human epithelial cell layer in vitro. Biochem. J. 377, 69–76. https://doi.org/10.1042/BJ20030760.
Liu, C., Tai, L., Zhang, W., Wei, G., Pan, W., Lu, W., 2014. Penetratin, a potentially powerful absorption enhancer for noninvasive intraocular drug delivery. Mol. Pharm. 11, 1218–1227. https://doi.org/10.1021/mp400681n.
Loftsson, T., Sigurdsson, H.H., Konrádsdóttir, F., Gísladóttir, S., Jansook, P., Stefánsson, E., 2008. Topical drug delivery to the posterior segment of the eye: Anatomical and physiological considerations. Pharmazie 63, 171–179. https://doi.org/10.1691/ph.2008.7322.
Lundin, P., Johansson, H., Guterstam, P., Holm, T., Hansen, M., Langel, Ü., Andaloussi, S. E.L., 2008. Distinct uptake routes of cell-penetrating peptide conjugates. Bioconjug. Chem. 19, 2535–2542. https://doi.org/10.1021/bc800212j.
Mahaling, B., Katti, D.S., 2016. Understanding the influence of surface properties of nanoparticles and penetration enhancers for improving bioavailability in eye tissues in vivo. Int. J. Pharm. 501, 1–9. https://doi.org/10.1016/j.ijpharm.2016.01.053.
Massa, H., Georgoudis, P., Panos, G.D., 2019. Dexamethasone intravitreal implant (OZURDEX®) for macular edema secondary to noninfectious uveitis: A review of the literature. Ther. Deliv. 10, 343–351. https://doi.org/10.4155/tde-2019-0024.
Milletti, F., 2012. Cell-penetrating peptides: Classes, origin, and current landscape. Drug Discov. Today 17, 850–860. https://doi.org/10.1016/j.drudis.2012.03.002.
Milojevic, Z., Agbaba, D., Eric, S., Boberic-Borojevic, D., Ristic, P., Solujic, M., 2002. High-performance liquid chromatographic method for the assay of dexamethasone and xylometazoline in nasal drops containing methyl p-hydroxybenzoate. J. Chromatogr. A 949, 79–82. https://doi.org/10.1016/S0021-9673(01)01510-2.
Moiseev, R.V., Morrison, P.W.J., Steele, F., Khutoryanskiy, V.V., 2019. Penetration enhancers in ocular drug delivery. Pharmaceutics 11, 321. https://doi.org/10.3390/pharmaceutics11070321.
Nicoli, S., Ferrari, G., Quarta, M., Macaluso, C., Govoni, P., Dallatana, D., Santi, P., 2009. Porcine sclera as a model of human sclera for in vitro transport experiments: histology, SEM, and comparative permeability. Mol. vis. 15, 259–266.
Oculis | Oculis Announces First Patient First Visit in Phase 3 OPTIMIZE-2 Trial of OCS-01 for the Treatment of Inflammation and Pain Following Cataract Surgery [WWW Document], n.d. URL https://investors.oculis.com/news-releases/news-release-details/oculis-announces-first-patient-first-visit-phase-3-optimize-2 (accessed 1.19.24).
Priegue, J.M., Lostalé-Seijo, I., Crisan, D., Granja, J.R., Fernández-Trillo, F., Montenegro, J., 2018. Different-Length Hydrazone Activated Polymers for Plasmid DNA Condensation and Cellular Transfection. Biomacromolecules 19, 2638–2649. https://doi.org/10.1021/acs.biomac.8b00252.
Ranta, V.P., Mannermaa, E., Lummepuro, K., Subrizi, A., Laukkanen, A., Antopolsky, M., Murtomäki, L., Hornof, M., Urtti, A., 2010. Barrier analysis of periocular drug delivery to the posterior segment. J. Control. Release 148, 42–48. https://doi.org/10.1016/j.jconrel.2010.08.028.
Richard, J.P., Melikov, K., Vives, E., Ramos, C., Verbeure, B., Gait, M.J., Chernomordik, L.V., Lebleu, B., 2003. Cell-penetrating peptides: A reevaluation of the mechanism of cellular uptake. J. Biol. Chem. 278, 585–590. https://doi.org/10.1074/jbc.M209548200.
Robinson, M.R., Lee, S.S., Kim, H., Kim, S., Lutz, R.J., Galban, C., Bungay, P.M., Yuan, P., Wang, N.S., Kim, J., Csaky, K.G., 2006. A rabbit model for assessing the ocular barriers to the transscleral delivery of triamcinolone acetonide. Exp. Eye Res. 82, 479–487. https://doi.org/10.1016/j.exer.2005.08.007.
Romero-Aroca, P., Baget-Bernaldiz, M., Pareja-Rios, A., Lopez-Galvez, M., Navarro-Gil, R., Verges, R., 2016. Diabetic Macular Edema Pathophysiology: Vasogenic versus Inflammatory. J. Diabetes Res. 2016, 1–17. https://doi.org/10.1155/2016/2156273.
Saincher, S.S., Gottlieb, C., 2020. Ozurdex (dexamethasone intravitreal implant) for the treatment of intermediate, posterior, and panuveitis: a systematic review of the current evidence. J. Ophthalmic Inflamm. Infect. 10, 1. https://doi.org/10.1186/s12348-019-0189-4.
Schoenwald, R.D., Ward, R.L., 1978. Relationship between steroid permeability across excised rabbit cornea and octanol-water partition coefficients. J. Pharm. Sci. 67, 786–788. https://doi.org/10.1002/jps.2600670614.
Shen, L., Fang, G., Tang, B., Zhu, Q., 2021. Enhanced topical corticosteroids delivery to the eye: A trade-off in strategy choice. J. Control. Release 339, 91–113. https://doi.org/10.1016/j.jconrel.2021.09.022.
Sigford, D.K., Reddy, S., Mollineaux, C., Schaal, S., 2015. Global reported endophthalmitis risk following intravitreal injections of anti-VEGF: A literature review and analysis. Clin. Ophthalmol. 9, 773–781. https://doi.org/10.2147/OPTH.S77067.
Sneddon, L.U., Halsey, L.G., Bury, N.R., 2017. Considering aspects of the 3Rs principles within experimental animal biology. J. Exp. Biol. 220, 3007–3016. https://doi.org/10.1242/jeb.147058.
Stefansson, E., Loftsson, T., Larsen, M., Papp, A., Kaarniranta, K., Munk, M.R., Dugel, P., Tadayoni, R., 2023. Topical treatment of diabetic macular edema using dexamethasone ophthalmic suspension: A randomized, double-masked, vehicle-controlled study. Acta Ophthalmol. 101, 22–33. https://doi.org/10.1111/aos.15215.
Stewart, A., Denoyer, D., Gao, X., Toh, Y.C., 2023. The FDA modernisation act 2.0: Bringing non-animal technologies to the regulatory table. Drug Discov. Today 28, 103496. https://doi.org/10.1016/J.DRUDIS.2023.103496.
Sugrue, S.P., Zieske, J.D., 1997. ZO1 in corneal epithelium: association to the zonula occludens and adherens junctions. Exp. Eye Res. 64, 11–20. https://doi.org/10.1006/exer.1996.0175.
Tahara, K., Karasawa, K., Onodera, R., Takeuchi, H., 2017. Feasibility of drug delivery to the eye's posterior segment by topical instillation of PLGA nanoparticles. Asian J. Pharm. Sci. 12, 394–399. https://doi.org/10.1016/j.ajps.2017.03.002.
Telander, D.G., 2011. Inflammation and age-related macular degeneration (AMD). Semin. Ophthalmol. 26, 192–197. https://doi.org/10.3109/08820538.2011.570849.
Thareja, A., Hughes, H., Alvarez-lorenzo, C., Hakkarainen, J.J., Ahmed, Z., 2021. Penetration enhancers for topical drug delivery to the ocular posterior segment — A systematic review. Pharmaceutics 13, 1–17. https://doi.org/10.3390/pharmaceutics13020276.
Thompson, J.T., 2006. Cataract formation and other complications of intravitreal triamcinolone for macular edema. Am. J. Ophthalmol. 141, 629–629.e10. https://doi.org/10.1016/j.ajo.2005.11.050.
Trier, K., 2005. The Sclera, Advances in Organ. Biology 353–373. https://doi.org/10.1016/S1569-2590(05)10013-5.
Ulrich, S., 2019. Growing prospects of dynamic covalent chemistry in delivery applications. Acc. Chem. Res. 52, 510–519. https://doi.org/10.1021/acs.accounts.8b00591.
Urtti, A., 2006. Challenges and obstacles of ocular pharmacokinetics and drug delivery. Adv. Drug Deliv. Rev. 58, 1131–1135. https://doi.org/10.1016/j.addr.2006.07.027.
Vakalis, N., Echiadis, G., Pervena, A., Deligiannis, I., Kavalarakis, E., Giannikakis, S., Papaefthymiou, I., 2015. Intravitreal combination of dexamethasone sodium phosphate and bevacizumab in the treatment of exudative AMD. Sci. Rep. 5, 8627. https://doi.org/10.1038/srep08627.

Vivès, E., Schmidt, J., Pèlegrin, A., 2008. Cell-penetrating and cell-targeting peptides in drug delivery. Biochim. Biophys. Acta - Rev. Cancer. https://doi.org/10.1016/j.bbcan.2008.03.001.

Walters, T., Endl, M., Elmer, T.R., Levenson, J., Majmudar, P., Masket, S., 2015. Sustained-release dexamethasone for the treatment of ocular inflammation and pain after cataract surgery. J. Cataract Refract. Surg. 41, 2049–2059. https://doi.org/10.1016/j.jcrs.2015.11.005.

Wang, Y., Xu, X., Gu, Y., Cheng, Y., Cao, F., 2018. Recent advance of nanoparticle-based topical drug delivery to the posterior segment of the eye. Expert Opin. Drug Deliv. 15, 687–701. https://doi.org/10.1080/17425247.2018.1496080.

Weijtens, O., Schoemaker, R.C., Romijn, F.P.H.T.M., Cohen, A.F., Lentjes, E.G.W.M., Van Meurs, J.C., 2002. Intraocular penetration and systemic absorption after topical application of dexamethasone disodium phosphate. Ophthalmology 109, 1887–1891. https://doi.org/10.1016/S0161-6420(02)01176-4.

Wen, H., Hao, J., Li, S.K., 2013. Characterization of human sclera barrier properties for transscleral delivery of bevacizumab and ranibizumab. J. Pharm. Sci. 102, 892–903. https://doi.org/10.1002/jps.23387.

Yang, X., Wang, L., Li, L., Han, M., Tang, S., Wang, T., Han, J., He, X., He, X., Wang, A., Sun, K., 2019. A novel dendrimer-based complex co-modified with cyclic RGD hexapeptide and penetratin for noninvasive targeting and penetration of the ocular posterior segment. Drug Deliv. 26, 989–1001. https://doi.org/10.1080/10717544.2019.1667455.